Supplementary Information

Deep learning for early warning signals of tipping points

Thomas M. Bury[1,2], R. I. Sujith[3], Induja Pavithran[4], Marten Scheffer[5], Timothy M. Lenton[6], Madhur Anand[2], Chris T. Bauch[1*]

1 Department of Applied Mathematics, University of Waterloo, Waterloo, Canada
2 School of Environmental Sciences, University of Guelph, Guelph, Canada
3 Department of Aerospace Engineering, Indian Institute of Technology Madras, Chennai, India
4 Department of Physics, Indian Institute of Technology Madras, Chennai, India
5 Department of Environmental Sciences, Wageningen University, Wageningen, The Netherlands
6 Global Systems Institute, University of Exeter, Exeter, UK

* cbauch@uwaterloo.ca

Contents

1 Supplementary Figures

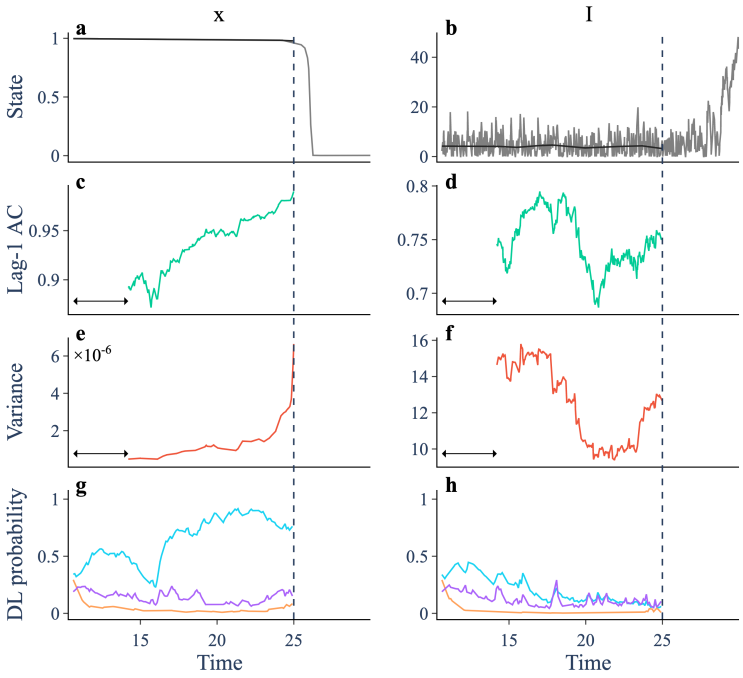

Supplementary Figure 1. Early warning signals and DL predictions prior to a vaccine scare in the SEIRx model. (a-b) Trajectory (grey) and smoothing (black) of a model simulation showing the vaccine uptake (x) and the proportion infected (I). The dashed vertical line identifies the onset of the transition. (c-d) Lag-1 autocorrelation computed over a rolling window (arrow) of size 0.25. (e-f) Variance. (g-h) Probabilities assigned to the fold (purple), Hopf (orange) and transcritical (cyan) bifurcation by the DL algorithm.

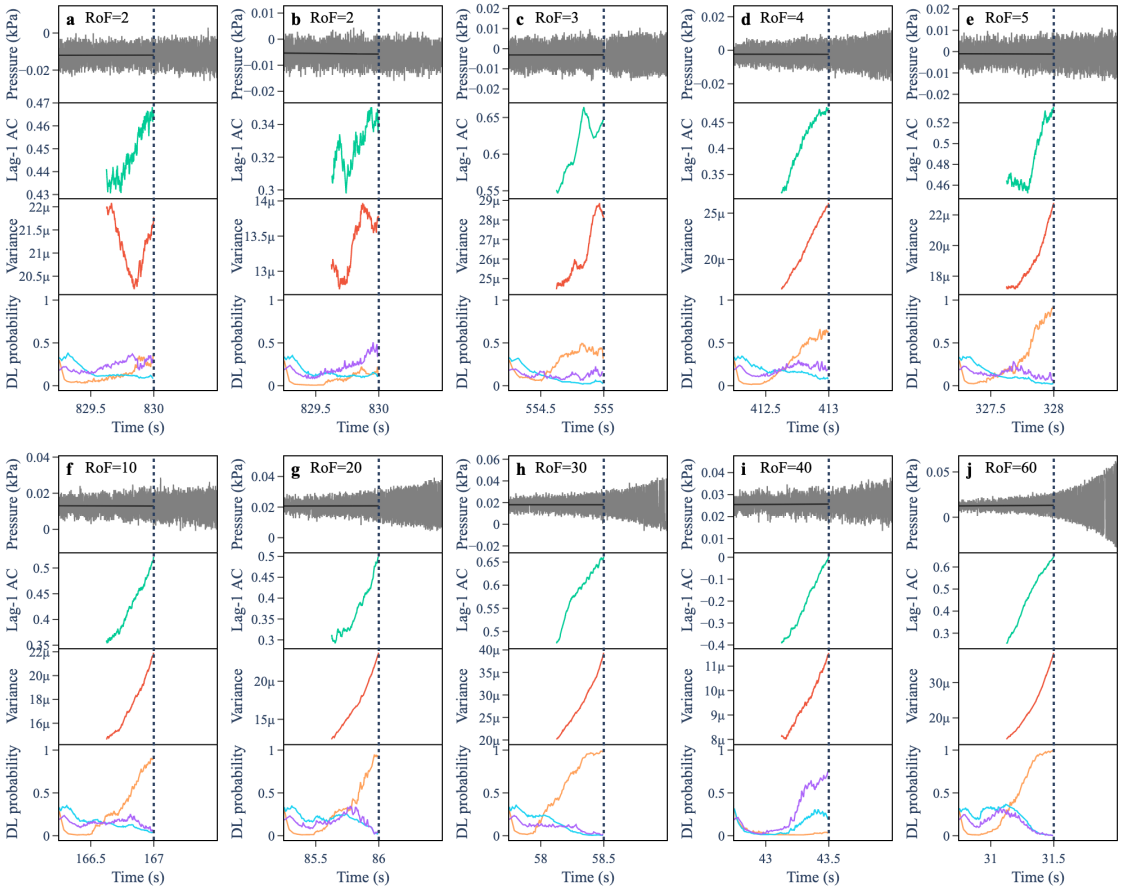

Supplementary Figure 2. Early warning signals and DL predictions for thermoacoustic transitions. (a-j) Each panel shows a thermoacoustic transition and leading indicators for a given rate of forcing (RoF) in mV/s. Note that two experiments with RoF=2 were conducted. (Top) Trajectory (grey) and smoothing (black). (2nd down) Lag-1 autocorrelation computed over a rolling window of length 0.5. (3rd down) Variance computed over a rolling window of length 0.5. (Bottom) Probabilities assigned to the fold (purple), Hopf (orange) and transcritical (cyan) bifurcation by the DL algorithm.

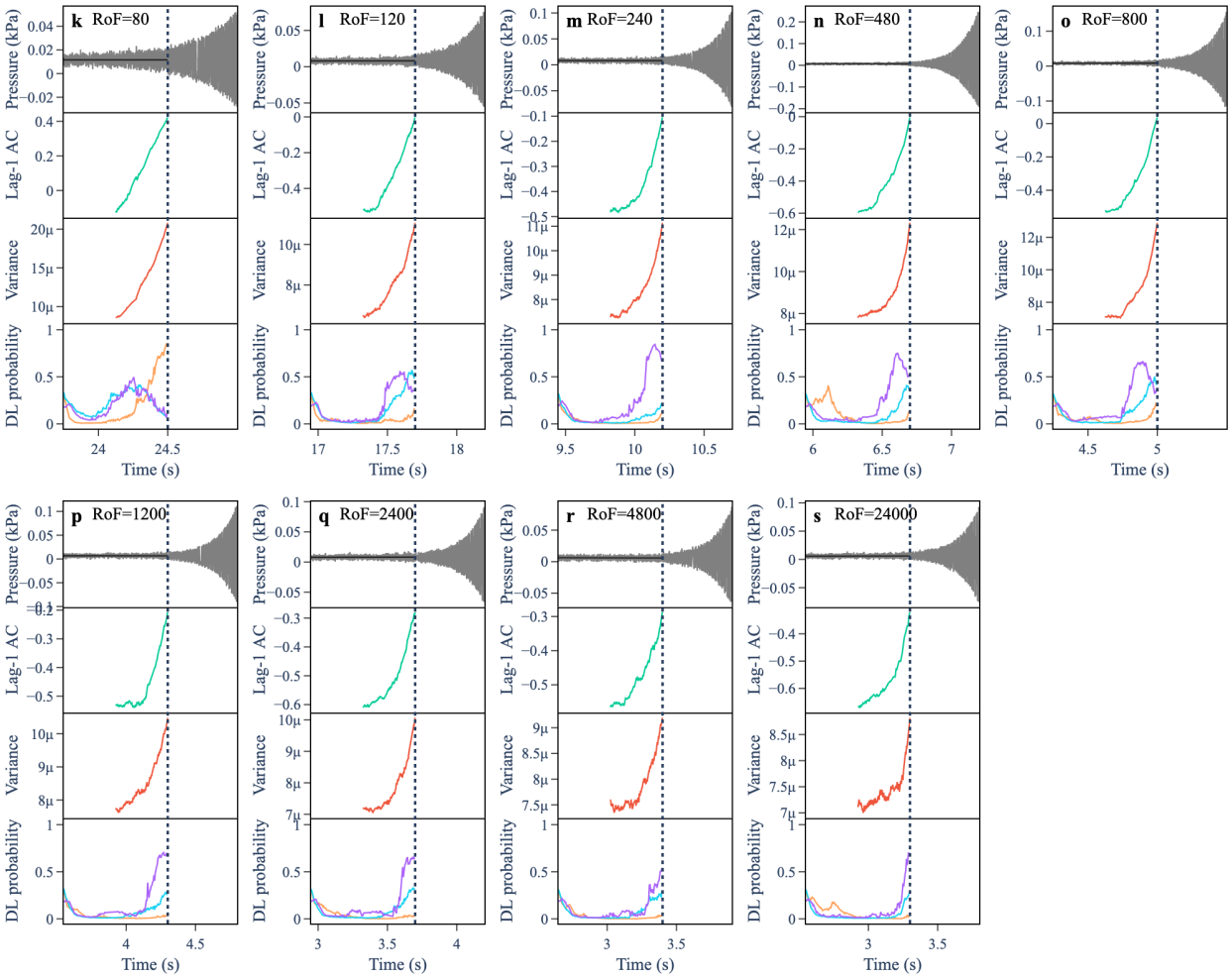

Supplementary Figure 3. Early warning signals and DL predictions for thermoacoustic transitions (continued). (k-s) Each panel shows a thermoacoustic transition and leading indicators for a given rate of forcing (RoF) in mV/s. (Top) Trajectory (blue) and Lowess smoothing (grey). (2nd down) Lag-1 autocorrelation computed over a rolling window of length 0.5. (3rd down) Variance computed over a rolling window of length 0.5. (Bottom) Probabilities assigned to the fold (purple), Hopf (orange) and transcritical (cyan) bifurcation by the DL algorithm.

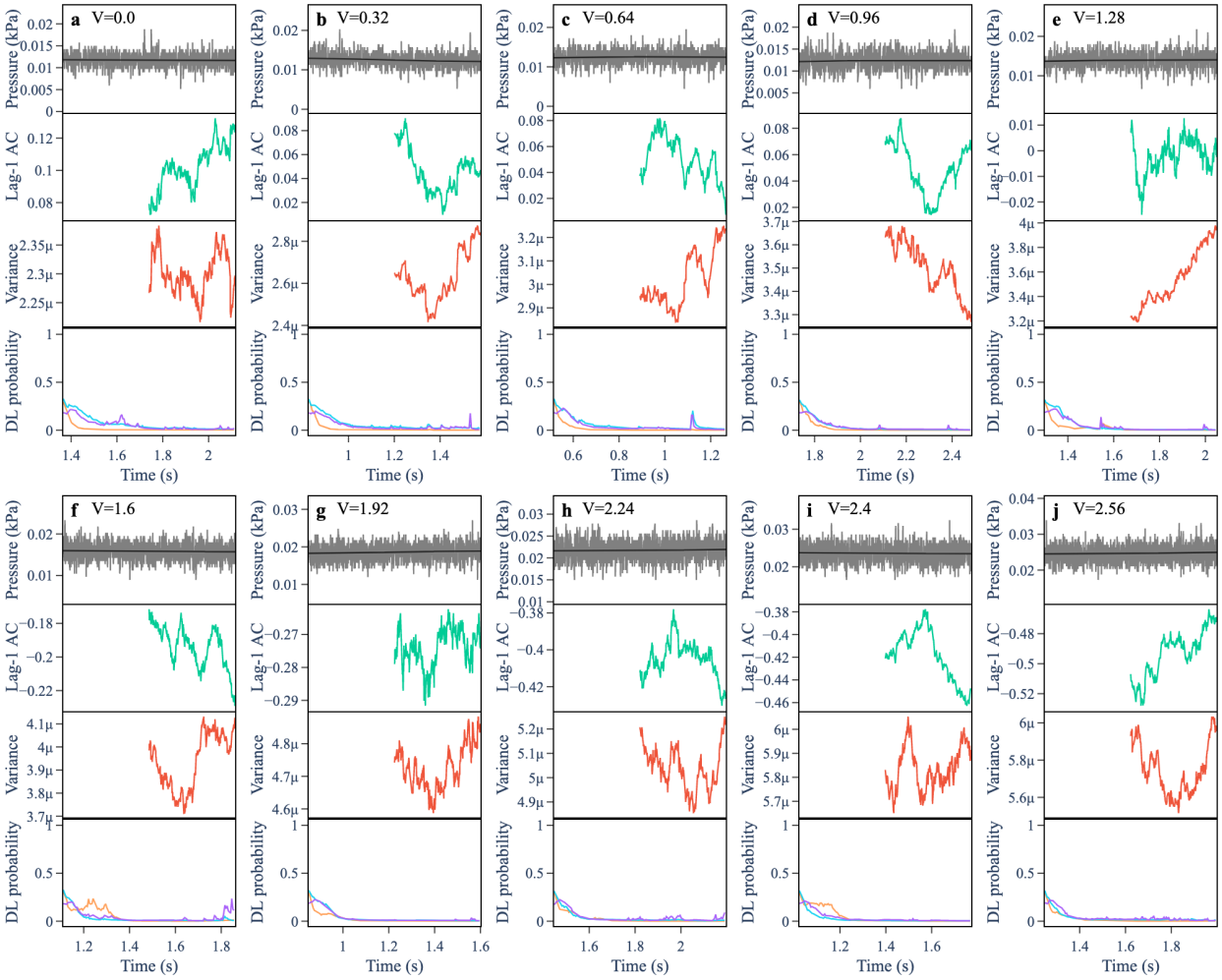

Supplementary Figure 4. Early warning signals and DL predictions for null thermoacoustic trajectories. (a-j) Each panel shows a thermoacoustic trajectory at some fixed voltage (V). (Top) Trajectory (blue) and Lowess smoothing (grey). (2nd down) Lag-1 autocorrelation computed over a rolling window of length 0.5. (3rd down) Variance computed over a rolling window of length 0.5. (Bottom) Probabilities assigned to the fold (purple), Hopf (orange) and transcritical (cyan) bifurcation by the DL algorithm.

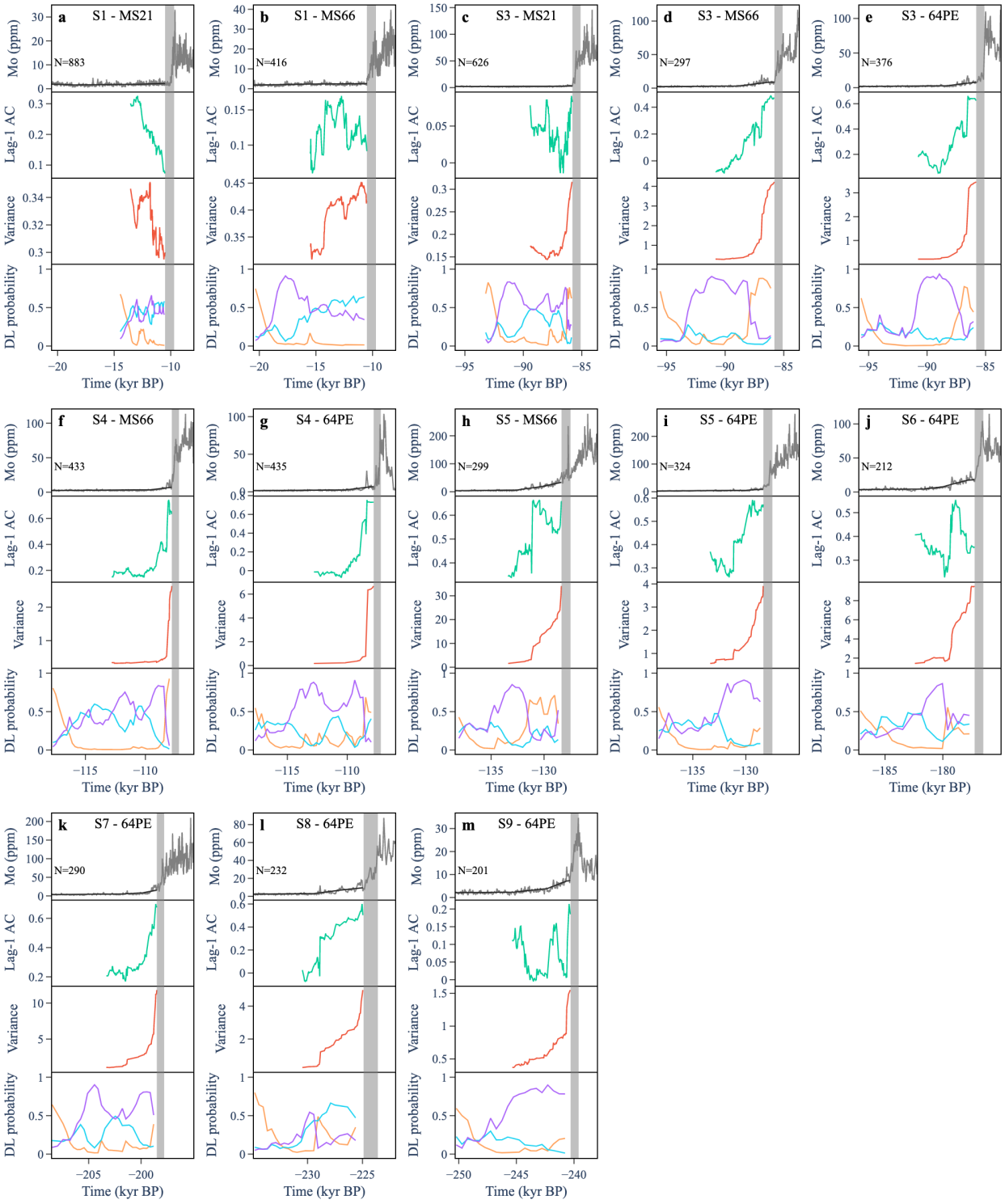

Supplementary Figure 5. Early warning signals and DL predictions in Molybdenum (Mo) data for 8 anoxic transitions. (a-m) Each panel shows a past anoxic transition (S1-S9) from data in a given core (MS21, MS66, or 64PE406E1). (Top) Trajectory (blue) and Gaussian smoothing (grey). (2nd down) Lag-1 autocorrelation computed over a rolling window of length 0.5. (3rd down) Variance computed over a rolling window of length 0.5. (Bottom) Probabilities assigned to the fold (purple), Hopf (orange) and transcritical (cyan) bifurcation by the DL algorithm.

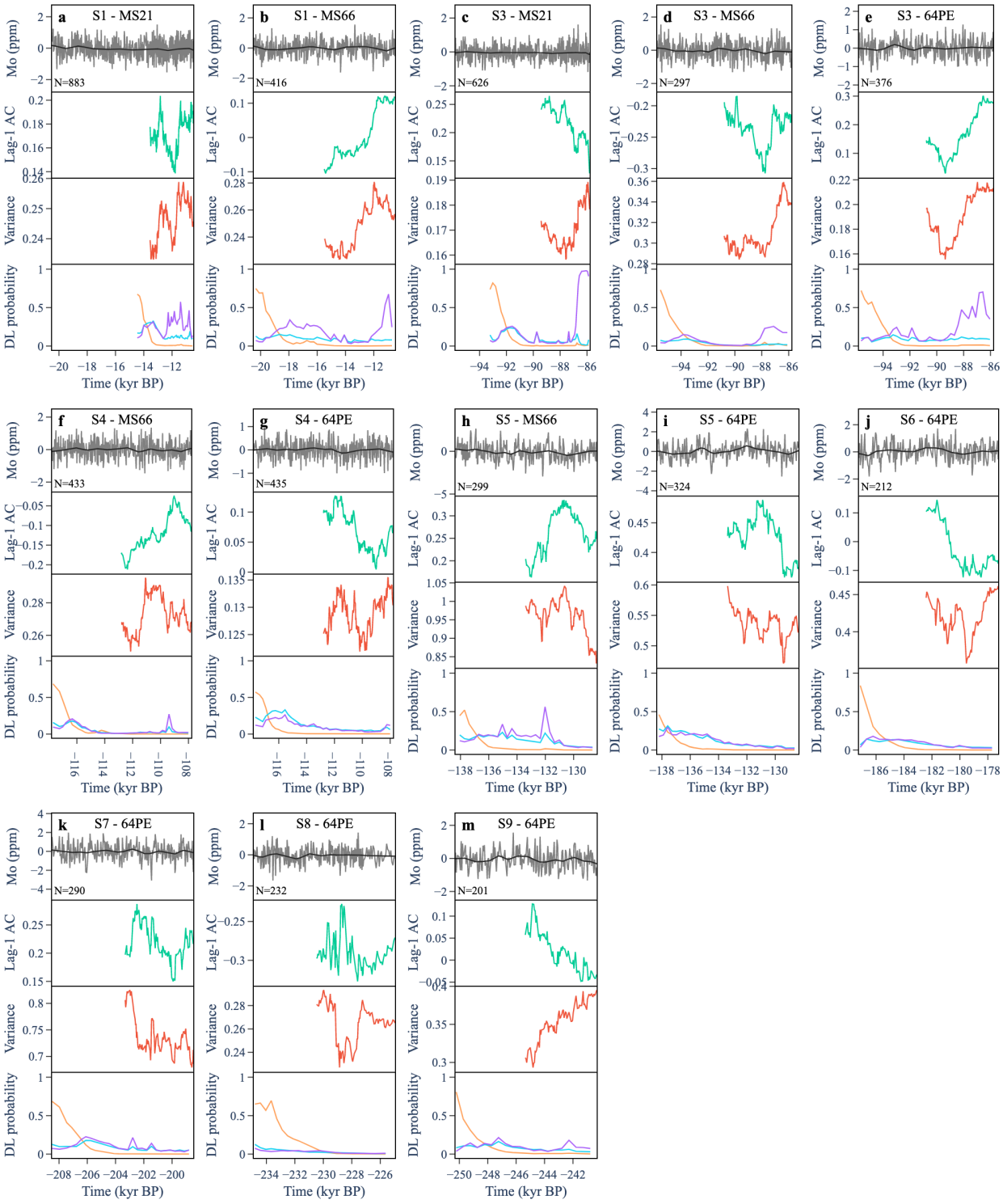

Supplementary Figure 6. Early warning signals and DL predictions for simulated null time series of Molybdenum (Mo). (a-m) Each panel shows a simulated null trajectory from an AR1 process fit to the first 20% of anoxic transitions (S1-S9) from data in a given core (MS21, MS66, or 64PE406E1). (Top) Trajectory (blue) and Gaussian smoothing (grey). (2nd down) Lag-1 autocorrelation computed over a rolling window of length 0.5. (3rd down) Variance computed over a rolling window of length 0.5. (Bottom) Probabilities assigned to the fold (purple), Hopf (orange) and transcritical (cyan) bifurcation by the DL algorithm.

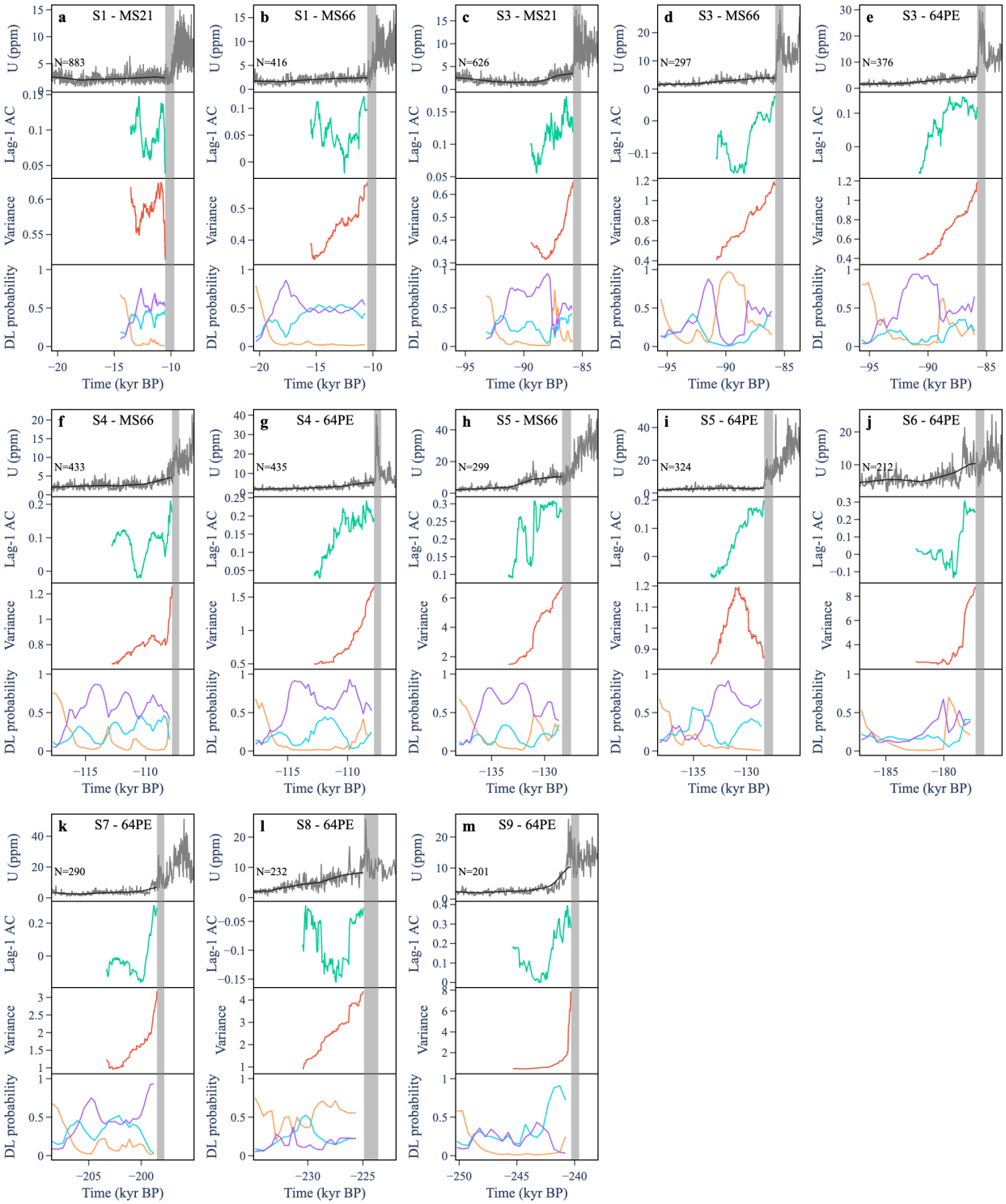

Supplementary Figure 7. Early warning signals and DL predictions in Uranium (U) data for 8 anoxic transitions. (a-m) Each panel shows a past anoxic transition (S1-S9) from data in a given core (MS21, MS66, or 64PE406E1). (Top) Trajectory (blue) and Gaussian smoothing (grey). (2nd down) Lag-1 autocorrelation computed over a rolling window of length 0.5. (3rd down) Variance computed over a rolling window of length 0.5. (Bottom) Probabilities assigned to the fold (purple), Hopf (orange) and transcritical (cyan) bifurcation by the DL algorithm.

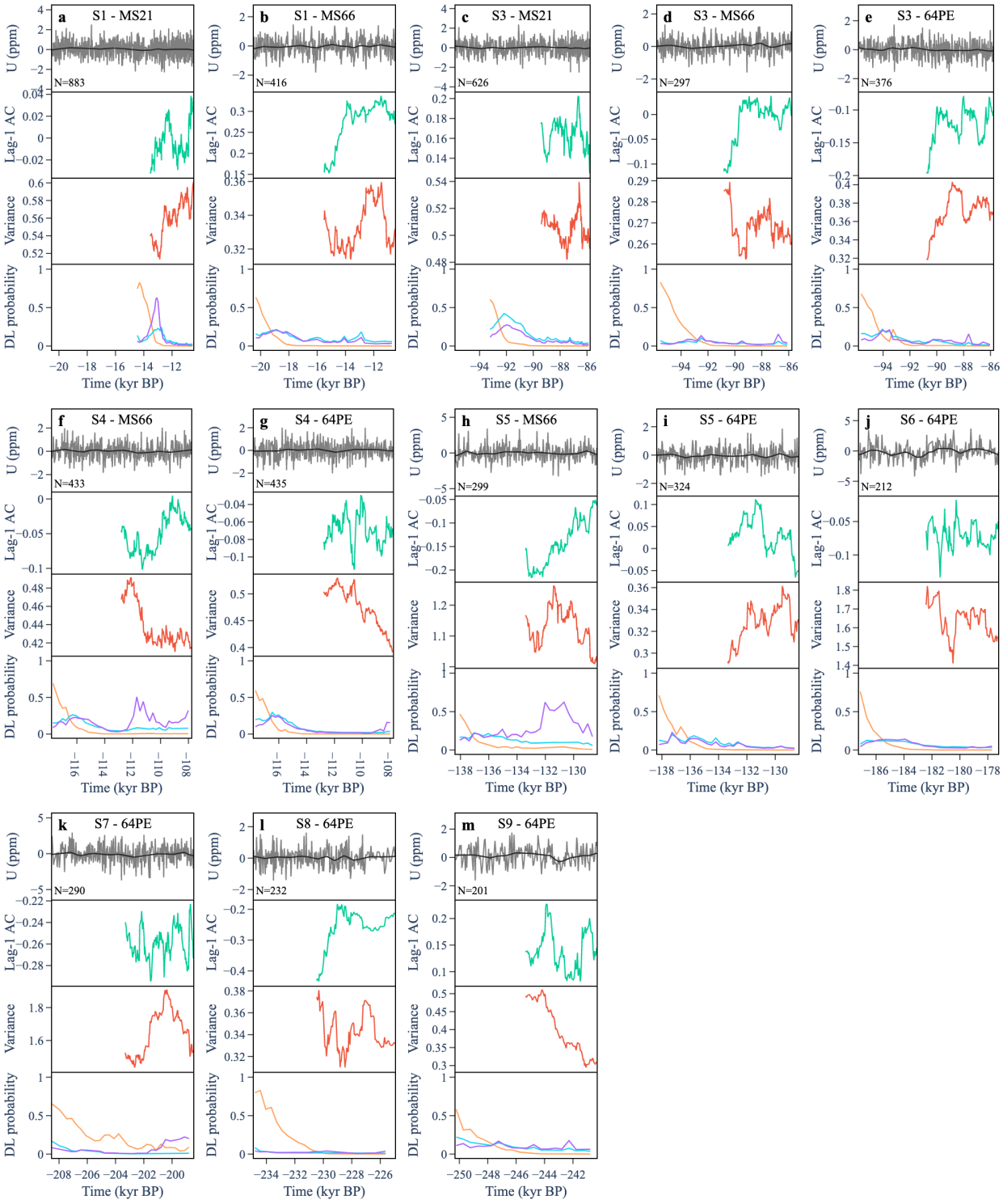

Supplementary Figure 8. Early warning signals and DL predictions for simulated null time series of Uranium (U). (a-m) Each panel shows a simulated null trajectory from an AR1 process fit to the first 20% of anoxic transitions (S1-S9) from data in a given core (MS21, MS66, or 64PE406E1). (Top) Trajectory (blue) and Gaussian smoothing (grey). (2nd down) Lag-1 autocorrelation computed over a rolling window of length 0.5. (3rd down) Variance computed over a rolling window of length 0.5. (Bottom) Probabilities assigned to the fold (purple), Hopf (orange) and transcritical (cyan) bifurcation by the DL algorithm.

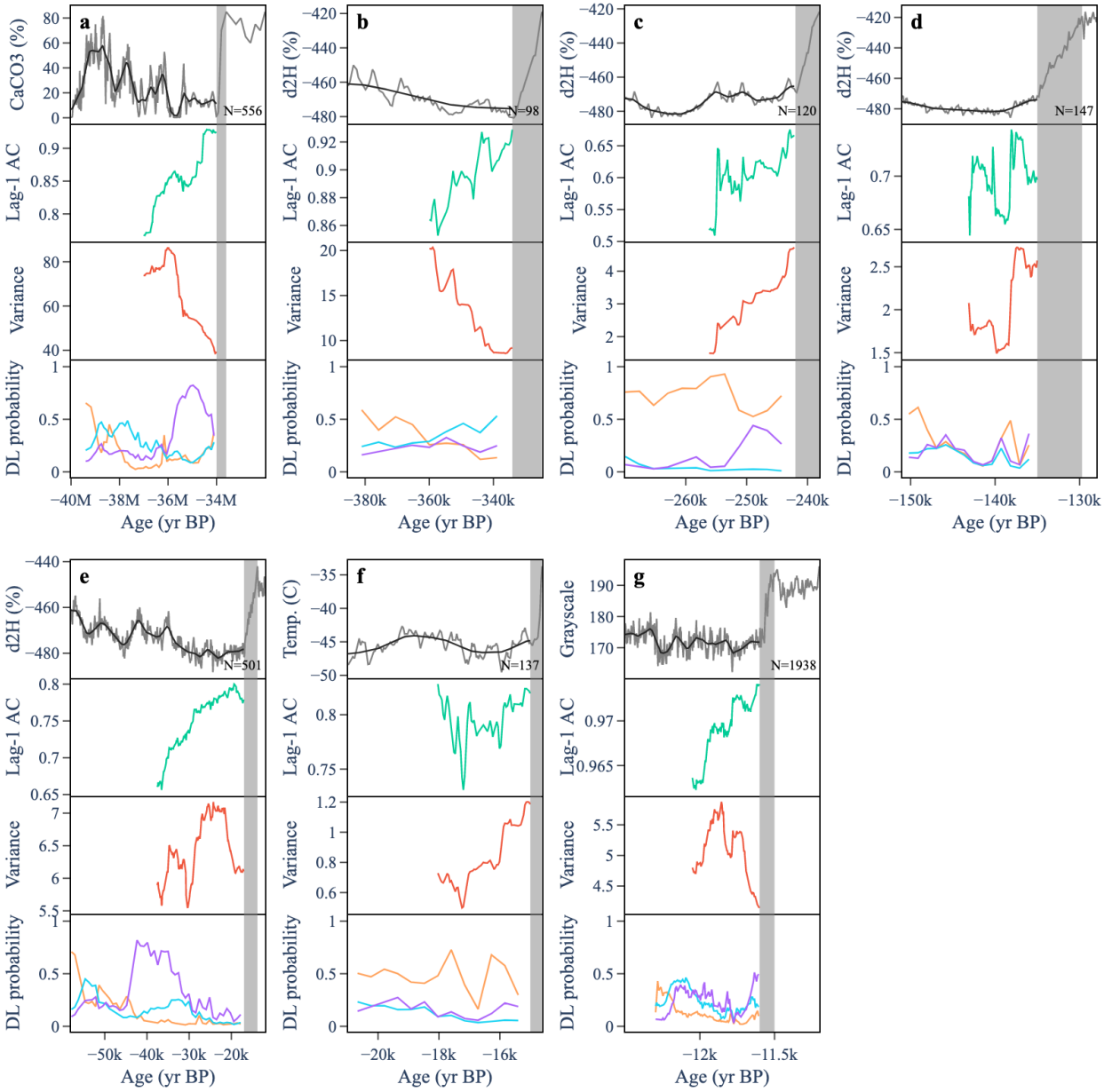

Supplementary Figure 9. Early warning signals and DL predictions for paleoclimate transitions. a) End of greenhouse Earth, b) End of glaciation IV, c) End of glaciation III, d) End of glaciation II, e) End of glaciation I, f) Bolling/Allerod transition, g) End of Younger Dryas. Panels are organised chronologically from oldest to youngest. (Top) Trajectory (blue) and Gaussian smoothing (grey). (2nd down) Lag-1 autocorrelation computed over a rolling window of length 0.5. (3rd down) Variance computed over a rolling window of length 0.5. (Bottom) Probabilities assigned to the fold (purple), Hopf (orange) and transcritical (cyan) bifurcation by the DL algorithm.

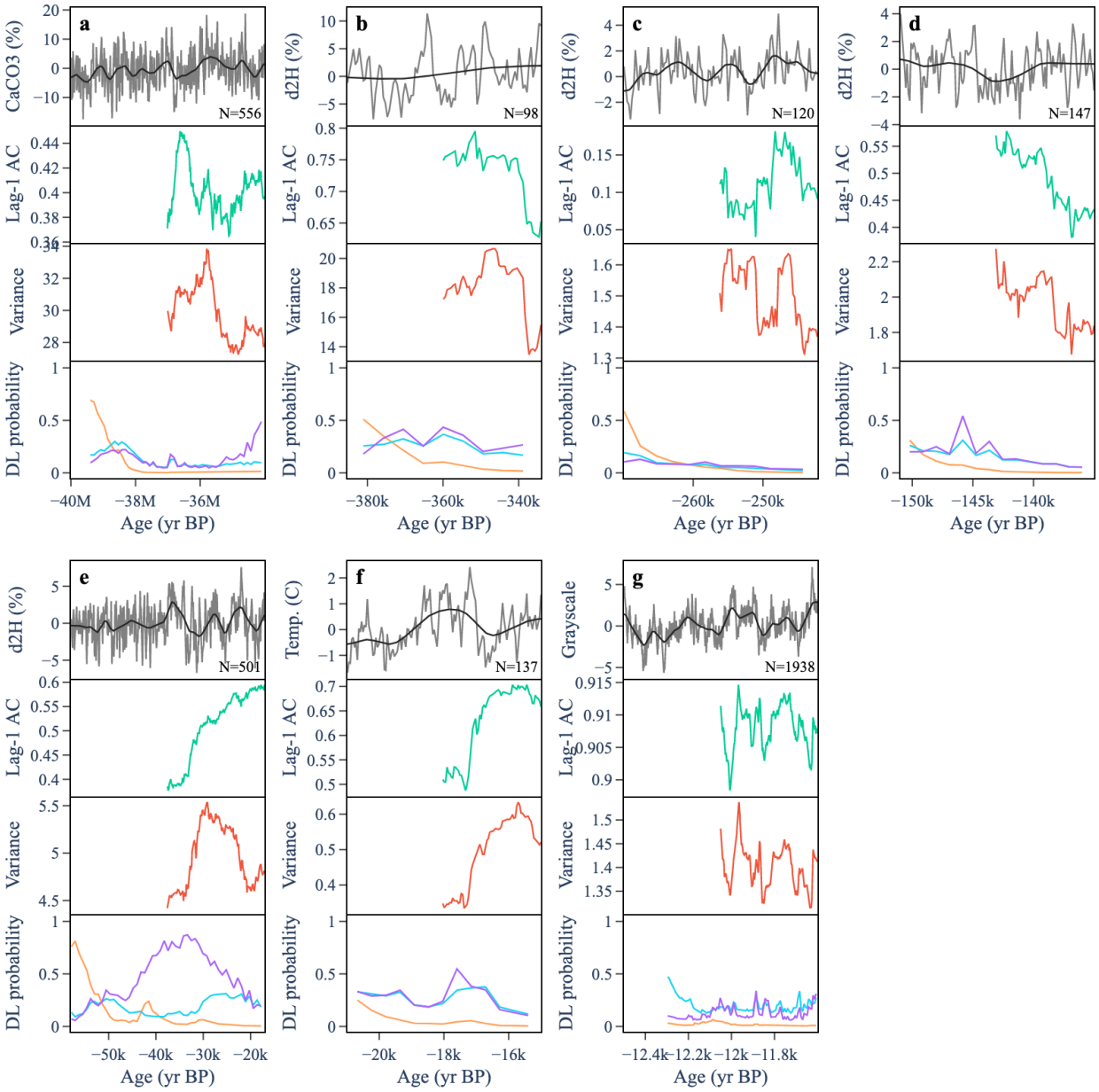

Supplementary Figure 10. Early warning signals and DL predictions in simulated null trajectories for paleoclimate data. a) End of greenhouse Earth, b) End of glaciation IV, c) End of glaciation III, d) End of glaciation II, e) End of glaciation I, f) Bolling/Allerod transition, g) End of Younger Dryas. Panels are organised chronologically from oldest to youngest. (Top) Trajectory (blue) and Gaussian smoothing (grey). (2nd down) Lag-1 autocorrelation computed over a rolling window of length 0.5. (3rd down) Variance computed over a rolling window of length 0.5. (Bottom) Probabilities assigned to the fold (purple), Hopf (orange) and transcritical (cyan) bifurcation by the DL algorithm.

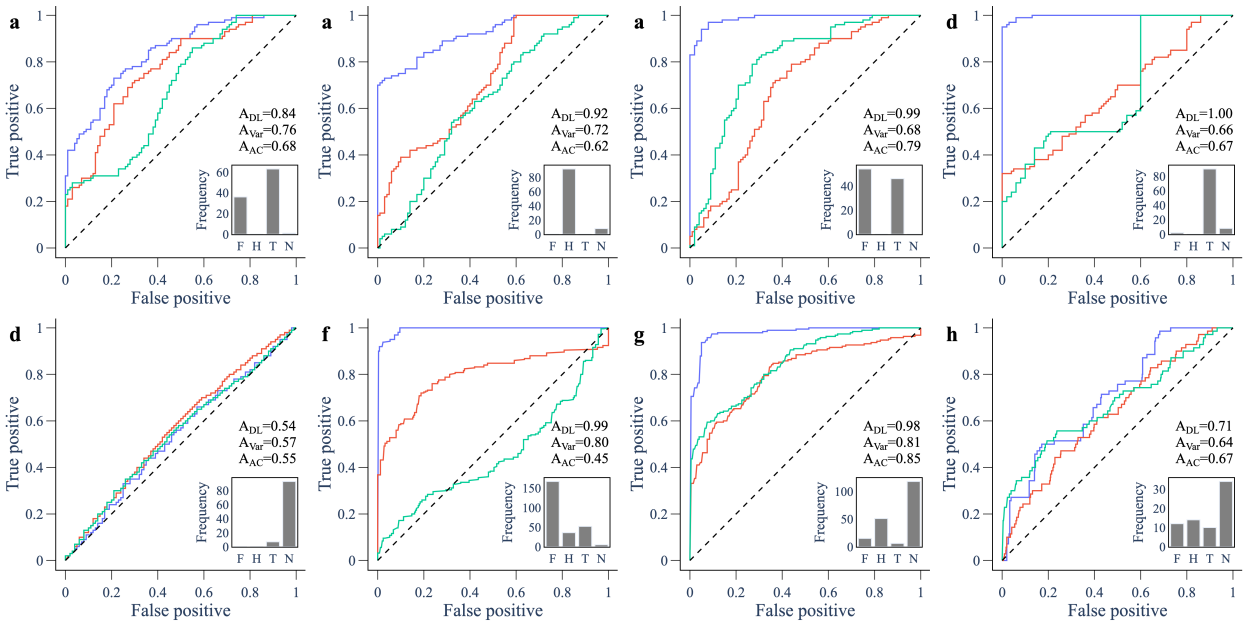

Supplementary Figure 11. ROC curves for predictions using 60% − 80% of the pre-transition time series for model and empirical data. ROC curves compare the performance of the DL algorithm (blue), variance (red) and lag-1 autocorrelation (green) in predicting an upcoming transition. The area under the curve (AUC), abbreviated to A, is a measure of performance. The inset shows the frequency of the favoured DL probability among the forced trajectories: (F)old, (T)transcritical, (H)opf, or (N)eutral. Panels show (**a**) May's harvesting model going through a fold bifurcation; consumer-resource model going through a (**b**) Hopf and (**c**) transcritical bifurcation; behaviour-disease model going through a transcritical bifurcation using data from (**d**) pro-vaccine opinion (x) and (**e**) total infectious (I); (**f**) sediment data showing rapid transitions to an anoxic states in the Mediterranean sea; (**g**) data of a thermoacoustic system undergoing a Hopf bifurcation; (**h**) ice core records showing rapid transitions in paleoclimate data.

2 Supplementary Note

2.1 Noise amplitude of simulations in training data

We would like to select a noise amplitude that lies in an appropriate range for each of the generated models. Ideally, simulations will have a noise amplitude that is large enough such that nonlinear terms are present in the signal, but small enough so that noise does not swamp the deterministic structure of the model. This amplitude is model-dependent, and can be approximated based on the size of the dominant eigenvalue of the generated model.

The framework that generates the models is two-dimensional. We chose to work with two-dimensional models since the normal form of each of the bifurcations considered has two dimensions or less. The normal forms may therefore be captured by our generic two-dimensional polynomial framework (Methods Eq. 4 and 5).

In a small neighbourhood of an equilibrium point, the dynamics of a training model are well described by its linearisation

$$\frac{d\vec{x}}{dt} = J\vec{x} + \sigma\vec{\xi}(t) \tag{1}$$

where $\vec{x} = (x, y)$ are the state variables, J is the Jacobian matrix, σ is the noise amplitude and $\vec{\xi(t)} = (\xi_1(t), \xi_2(t))$ are the white noise processes. This equation describes an Ornstein-Uhlenbeck process, for which the variance can be computed analytically [1]. To first-approximation, this variance is given by

$$\text{Var} \approx \frac{\sigma^2}{2|\text{Re}(\lambda)|} \tag{2}$$

where λ is the dominant eigenvalue of J, that is, the eigenvalue whose real part has the smallest magnitude. The dominant eigenvalue can be computed for each dynamical system that we generate. This approximate relationship is shown by simulating an ensemble of models with fixed, small noise $\sigma = 0.01$, and plotting the variance against the size of the dominant eigenvalue (Figure 12).

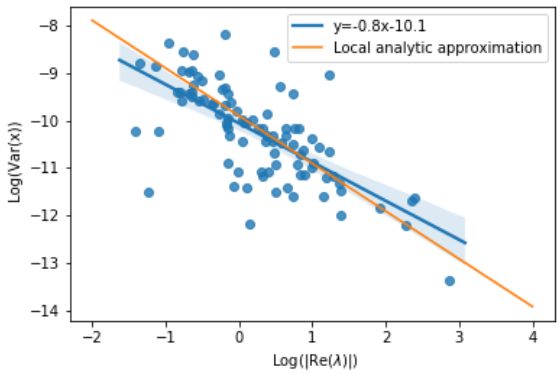

Supplementary Figure 12. Relationship between variance of a stationary realisation and its dominant eigenvalue. The local analytic approximation is the expression in Eqn. (2). This shows good agreement with numerical simulations.

In order to control for the variance of simulations across the initial parameter configuration of each system, we need to scale σ accordingly. We therefore take the noise amplitude for each model to be

$$\sigma = \sqrt{2|\text{Re}(\lambda)|}\tilde{\sigma}T, \tag{3}$$

where $\tilde{\sigma} = 0.01$ and T is drawn from the triangular distribution $T \in \mathcal{T}(0.75, 1, 1.25)$.

References

1. Gardiner, C. W. *et al. Handbook of stochastic methods* (Springer Berlin, 1985).